J|A|C|S
ARTICLES
Published on Web 01/17/2002

# Synthesis and Characterization of Pt(CN-*p*-$(C_2H_5)C_6H_4)_2(CN)_2$, a Crystalline Vapoluminescent Compound That Detects Vapor-Phase Aromatic Hydrocarbons

Carrie E. Buss and Kent R. Mann*

*Contribution from the Department of Chemistry, University of Minnesota, Minneapolis, Minnesota 55455*

Received August 16, 2001

***Abstract:*** The vapochromic and vapoluminescent compound Pt(CN-*p*-$(C_2H_5)C_6H_4)_2(CN)_2$ (abbreviated **$PtC_2$**) is conveniently synthesized by the thermal rearrangement of [Pt(CN-*p*-$(C_2H_5)C_6H_4)_4$][$Pt(CN)_4$]. Recrystallization of **$PtC_2$** gives a crystalline orange morph (**O-$PtC_2$**) and an amorphous purple morph (**P-$PtC_2$**) that both contain the cis isomer and differ only in their solid-state packing arrangements. Both compounds were fully characterized by elemental analysis, X-ray powder diffraction, NMR, IR, and TGA. **O-$PtC_2$** is vapochromic and vapoluminescent: it reversibly sorbs aromatic hydrocarbons and ethanol from air or nitrogen with resulting color changes and shifts in the emission spectrum. The $\lambda_{max}$ values (nm) for emission from **O-$PtC_2$**·(guest) are as follows: no guest, 611; toluene, 565; benzene, 586; chlorobenzene, 592; *p*-xylene, 585; mesitylene, 565; ethanol, 587. In the case of toluene and mesitylene, intermediate emitting phases are observed. Recrystallization of **O-$PtC_2$** from dichloromethane/toluene gave single crystals of **$PtC_2$**·0.5(toluene). The single-crystal X-ray structure of **$PtC_2$**·0.5(toluene) contains infinite stacks of cis geometry and planar molecules with chains of platinum atoms parallel to the *c* axis of the monoclinic unit cell. The average Pt−Pt separation in **$PtC_2$**·0.5(toluene) is $c/4 = 3.288(2)$ Å. There are solvent channels parallel with the *c* axis that contain the toluene molecule guests. Thin films of **O-$PtC_2$** rapidly sorb toluene from the gas phase to form **$PtC_2$**·0.25(toluene) and **$PtC_2$**·0.5(toluene). Long-term exposure gives **$PtC_2$**·1.0(toluene). Removal of the toluene source causes rapid desorption to **$PtC_2$**·0.5(toluene) and then to **$PtC_2$**·0.25(toluene). The remaining 0.25(toluene) lattice guests require heating for rapid removal. X-ray powder diffraction identified the **$PtC_2$**, **$PtC_2$**·0.25(toluene), and **$PtC_2$**·0.5(toluene) phases and showed that the sorption of toluene is accompanied by small changes in the unit cell dimensions that include lengthening the Pt−Pt distances in the structure. The sorption process improves the packing in the structure by utilizing some of the free volume for the toluene lattice guests.

## Introduction

The development of reversible chemical sensor materials with high stability has received increasing attention.[1] Materials that show dramatic and reversible color changes in the visible or near-infrared (near-IR) spectral regions upon exposure to volatile organic compounds (VOCs) are of particular interest.[2−5] To be useful, such materials should not only detect VOCs at low levels but should also show a unique response for each VOC. Several compounds of this type could also be used as a sensor array in an "electronic nose"[6] or as the detecting or emitting layer in a photodiode or in a LED.[7−9]

Our previous studies of square-planar $d^8$ platinum compounds of the form [$Pt(CNR)_4$][$M(CN)_4$] (M = Pt, Pd; R = aryl, alkyl; "double salts") have shown that they can form the chemically sensitive layer for such a chemical sensor system.[10−14] In general, the complexes are robust and form intensely colored solid-state materials that reversibly sorb solvent molecules from

* To whom correspondence should be addressed.

(1) A literature search produced several thousand references in the general area of sensors published between 1996 and 2000.
(2) Mansour, M. A.; Connick, W. B.; Lachicotte, R. J.; Gysling, H. J.; Eisenberg, R. *J. Am. Chem. Soc*. **1998**, *120*, 1329.
(3) Beauvais, L. G.; Shores, M. P.; Long, J. R. *J. Am. Chem. Soc*. **2000**, *122*, 2763.
(4) Cariati, E.; Bu, X.; Ford, P. C. *Chem. Mater*. **2000**, *12*, 3385.
(5) Evju, J. K.; Mann, K. R. *Chem. Mater*. **1999**, *11*, 1425.
(6) (a) Drew, S. M.; Janzen, D. E.; Buss, C. E.; MacEwan, D. I.; Dublin, K. I.; Mann, K. R. *J. Am. Chem. Soc*. **2001**, *123*, 8414. (b) Gardner, J. W.; Bartlett, P. N. *Electronic Noses: Principles and Applications*; Oxford University Press: New York, 1999. (c) Persaud, K.; Dodd, G. H. *Nature (London)* **1982**, *299*, 352. (d) Albert, K. J.; Lewis, N. S.; Schauer, C. L.; Sotzing, G. A.; Stitzel, S. E.; Vaid, T. P.; Walt, D. R. *Chem. Rev*. **2000**, *100*, 2595−2626. (e) Grate, J. W. *Chem. Rev*. **2000**, *100*, 2627−2648. (f) Lundstrom, I.; Hedborg, E.; Spetz, A.; Sundgren, H.; Winquist, F. Electronic Nose Based on Field Effect Structures. In *Sensors and Sensory Systems for an Electronic Nose*; Gardner, J. W., Bartlett, P. N., Eds.; NATO ASI Series 212; Kluwer: Dordrecht, The Netherlands, 1992; pp 303−319. (g) Miller, L. L.; Boyd, D. C.; Schmidt, A. J.; Nitzkowski, S. C.; Rigaut, S. *Chem. Mater*. **2001**, *13*, 9−11. (h) Dickinson, T. A.; White, J.; Kauer, J. S.; Walt, D. R. *Nature* **1996**, *382*, 697−700. (i) Rakow, N. A.; Suslick, K. S. *Nature* **2000**, *406*, 710−713. (j) Seker, F.; Meeker, K.; Kuech, T. F.; Ellis, A. B. *Chem. Rev*. **2000**, *100*, 2505−2536. (k) Sohn, H.; Letant, S.; Sailor, M. J.; Trogler, W. C. J. *Am. Chem. Soc*. **2000**, *122*, 5399−5400. (l) Additional references are given in the Supporting Information.
(7) Kunugi, Y.; Mann, K. R.; Miller, L. L.; Pomije, M. K. (Regents of the University of Minnesota) U.S. Patent 6,137,118, 2000.
(8) Kunugi, Y.; Mann, K. R.; Miller, L. L.; Exstrom, C. L. (Regents of the University of Minnesota) U.S. Patent 6,160,267, 2000.
(9) Kunugi, Y.; Miller, L. L.; Mann, K. R.; Pomije, M. K. *Chem. Mater*. **1998**, *10*, 1487.
(10) Daws, C. A.; Exstrom, C. L.; Sowa, J. R.; Mann, K. R. *Chem. Mater*. **1997**, *9*, 363.
(11) Exstrom, C. L.; Pomije, M. K.; Mann, K. R. *Chem. Mater*. **1998**, *10*, 942.

the gas phase, a process that is coupled with a shift in the absorption spectrum. This process has been termed vapochromism[15] and is accompanied by reversible physical changes.[10−14] The vapochromic phenomenon has been studied with a variety of techniques that include FT-IR, UV−vis absorption and emission spectroscopy, solid-state NMR, powder and single-crystal X-ray diffraction, and thermal gravimetric analysis. Vapochromism in crystalline $[Pt(CNR)_4][Pt(CN)_4]$ salts arises from highly anisotropic packing forces that enable solvent vapors to reversibly penetrate the interior of the material to form a new crystalline phase with precisely determined solvent−chromophore interactions.[10−14] The $[Pt(CNR)_4][Pt(CN)_4]$ solids consist of infinite stacks of alternating $Pt(CNR)_4^{2+}$ dications and $Pt(CN)_4^{2-}$ dianions. The interionic metal−metal interactions produce the chromophore.[10−14] The vapor inclusion causes color changes that result from a combination of chemical interactions with the chromophore, including changes in the dielectric constant near the chromophore, hydrogen bonding between the solvent and coordinated cyanide, and expansion or contraction of the unit cell that is coupled to the Pt−Pt distance.

When the double-salt compounds $[Pt(CNR)_4][Pt(CN)_4]$ are exposed to liquid chlorinated solvents for long periods of time (days) or are heated to the melting point in the absence of solvent, a ligand rearrangement reaction forms the isomeric neutral compounds $Pt(CNR)_2(CN)_2$.[16] These neutral compounds are interesting because they also exhibit vapochromic properties, have enhanced thermal stability, and have favorable solubility properties. This paper reports a well-characterized example ($Pt(CN\text{-}p\text{-}(C_2H_5)C_6H_4)_2(CN)_2$) of this neutral compound class that illustrates some aspects of their sensing capabilities.

## Experimental Section

**General Considerations.** 4-Ethylaniline was purchased from Aldrich Chemical Co. Elemental analyses were performed by Quantitative Technologies Inc. Analytical Laboratories. $Pt(CH_3CN)_2Cl_2$ was prepared from $K_2[PtCl_4]$ (Colonial Metals) as previously reported.[17] $[(n\text{-}C_4H_9)_4N]_2[Pt(CN)_4]$ was prepared from $[(n\text{-}C_4H_9)_4N]Br$ (Aldrich) and $K_2[Pt(CN)_4]$ (Colonial Metals) as previously reported.[18] All solvents used in the IR and UV−vis studies were ACS reagent grade and dried over molecular sieves prior to use.

**Materials. $p$-$(C_2H_5)C_6H_4$-NHCHO.** A mixture of $p$-$(C_2H_5)C_6H_4$-$NH_2$ (10.3 mL, 0.0825 mol), 88% formic acid (30 mL, 0.82 mol), and toluene (100 mL) was stirred at reflux for 9 h in a round-bottom flask equipped with a condenser and a Dean−Stark water separator. Cooling the mixture to room temperature afforded white flakes of $p$-$(C_2H_5)$-$C_6H_4$-NHCHO that were separated from the mixture by filtration. A second crop of the formamide was obtained by concentrating the filtrate under vacuum to give a total of 10.749 g (87% yield). $^1$H NMR ($CDCl_3$): $\delta$ 8.63 (d, $E$ isomer, $^1/_2$ H, CHO), 8.48 (br d, $Z$ isomer, $^1/_2$ H, NH), 8.32 (d, $Z$ isomer, $^1/_2$ H, CHO), 7.58 (br s, $E$ isomer, $^1/_2$ H, NH), 7.43 (m, 1H, Ph), 7.15 (m, 2H, Ph), 7.00 (m, 1H, Ph), 2.60 (m, 2H, $CH_2$), 1.20 (m, 3H, $CH_3$). IR (ATR ZnSe crystal): $\nu_{CO}$ ($cm^{-1}$) 1679 vs.

**$p$-$(C_2H_5)C_6H_4$-NC.** The aryl isocyanide was prepared from the corresponding amine by dehydrating the formamide compound via a slight modification of the method of Ugi and Meyr.[19] Triethylamine was dried over 3 Å molecular sieves and passed through a short column of activated alumina immediately prior to use. A mixture of $p$-$(C_2H_5)$-$C_6H_4$-NHCHO (5.695 g, 38.17 mmol), triethylamine (26.6 mL, 190.8 mmol), and $CH_2Cl_2$ (100 mL) was cooled to 0 °C in an ice bath. With stirring, $POCl_3$ (3.91 mL, 41.9 mmol) was added to the mixture dropwise over a 30 min period. The mixture was stirred at 0 °C for 30 min, during which the solution color gradually turned from pale yellow to orange-brown. The ice−water bath was removed, and 100 mL of a phosphate buffer (pH 6.3) solution was added dropwise over a period of 30 min. The organic layer was removed in a separatory funnel, washed (3 × 100 mL) with a saturated NaCl solution, and dried over anhydrous $CaCl_2$. The $CaCl_2$ was removed via filtration, and the solvent was removed in vacuo to yield a dark brown liquid (4.724 g, 94%). $^1$H NMR ($CD_2Cl_2$): $\delta$ 7.29 (d, 2 H, Ph), 7.21 (d, 2 H, Ph), 2.66 (q, 2 H, $CH_2$), 1.21 (t, 3 H, $CH_3$). $^{13}$C NMR ($CD_2Cl_2$): $\delta$ 164.28 (CNR), 146.66 (Ph), 129.34 (Ph), 126.77 (Ph), 124.91 (Ph), 29.13 ($CH_2$), 15.60 ($CH_3$); IR (ATR ZnSe crystal) $\nu_{CN}$ ($cm^{-1}$) 2122 vs.

**$[Pt(p\text{-}CN\text{-}C_6H_4C_2H_5)_4][Pt(CN)_4]$[20] (4C$_2$).** This compound was previously made by Keller and Lorentz by an alternate method.[21] A better procedure described for preparing $[Pt(p\text{-}CN\text{-}C_6H_4C_{10}H_{21})_4][Pt(CN)_4]$[19] was followed: $Pt(CH_3CN)_2Cl_2$ (1.19 g, 3.43 mmol), $[(n\text{-}C_4H_9)_4N]_2[Pt(CN)_4]$ (2.69 g, 3.43 mmol), and $p$-CN-$C_6H_4C_2H_5$ (2.24 g, 17.1 mmol) in acetonitrile (150 mL) were stirred for 1.0 h to yield a blue precipitate that was isolated by filtration (3.01 g, 86% yield). Mp: 201 °C dec. IR (ATR ZnSe crystal): $\nu_{CNR}$ 2258 $cm^{-1}$ (vs); $\nu_{CN}$ 2126 $cm^{-1}$ (vs). Near-IR (ATR ZnSe crystal): $\lambda_{max}$ 876 nm. Anal. Calcd for $C_{20}H_{18}N_4Pt$: C, 47.15; H, 3.56; N, 11.00. Found: C, 46.40; H, 3.32; N, 10.59.

**Purple $Pt(p\text{-}CN\text{-}C_6H_4C_2H_5)_2(CN)_2$ (P-PtC$_2$).** The neutral compound was synthesized by heating $[Pt(p\text{-}CN\text{-}C_6H_4C_2H_5)_4][Pt(CN)_4]$ (0.772, 0.758 mmol) under an argon atmosphere to the melting point. When the mixture was cooled, a glassy orange-red solid that is soluble in $CH_2Cl_2$ was obtained. Recrystallization from $CH_2Cl_2$ and excess hexanes led to a purple powder (0.589 g, 1.16 mmol, 76%). $^1$H NMR ($CD_2Cl_2$): $\delta$ 7.51 (d, 2 H, Ph), 7.36 (d, 2 H, Ph), 2.74 (q, 2 H, $CH_2$), 1.25 (t, 3 H, $CH_3$). IR (ATR ZnSe crystal): $\nu_{CNR}$ 2251 (vs), 2231 $cm^{-1}$ (vs); $\nu_{CN}$ 2157 (vs), 2150 $cm^{-1}$ (vs). UV−vis (ATR, cubic zirconia crystal): $\lambda_{max}$ 570 nm. Mp: 143 °C. Anal. Calcd for $C_{20}H_{18}N_4Pt$: C, 47.15; H, 3.56; N, 11.00. Found: C, 46.99; H, 3.52; N, 10.75.

**Orange $Pt(p\text{-}CN\text{-}C_6H_4C_2H_5)_2(CN)_2$ (O-PtC$_2$).** O-PtC$_2$ was obtained by the slow recrystallization of **P-PtC$_2$** from acetone/ether but the procedure was prone to produce material contaminated with **P-PtC$_2$**. A better method was to slurry a sample of **P-PtC$_2$** (obtained by the method above) with THF to give a yellow solid. Removal of the THF solvent followed by heating to 100 °C yielded the orange product upon cooling. Both procedures gave products that are identical by NMR and FTIR. $^1$H NMR ($CD_2Cl_2$): $\delta$ 7.52 (d, 2 H, Ph), 7.36 (d, 2 H, Ph), 2.74 (q, 2 H, $CH_2$), 1.25 (t, 3 H, $CH_3$). $^{13}$C NMR ($CD_2Cl_2$): $\delta$ 171.61 (CNR), 149.50 (Ph), 129.75 (Ph), 127.61 (Ph), 123.28 (Ph), 110.67 (CN) with satellite peaks at $\delta$ 118.14 and 103.22 ($J(^{195}Pt-^{13}C) = 562.8$ Hz), 29.31 ($CH_2$), 15.38 ($CH_3$). IR (ATR ZnSe crystal): $\nu_{CNR}$ 2247 (vs), 2229 $cm^{-1}$ (vs); $\nu_{CN}$ 2157 (vs), 2150 $cm^{-1}$ (vs). UV−vis (thin film transmission): $\lambda_{max}$ 515 nm. Mp: 174 °C. Anal. Calcd for $C_{20}H_{18}N_4Pt$: C, 47.15; H, 3.56; N, 11.00. Found: C, 47.09; H, 3.58; N, 10.76.

**Gravimetric Measurements.** Solvent uptake/release studies were conducted by thermal gravimetric analysis (TGA) with a Perkin-Elmer TGA 7 instrument or by gravimetric analysis (Acculab LA-60 electronic balance). TGA measurements were conducted with both **P-PtC$_2$** and **O-PtC$_2$** in the unexposed state to determine if any lattice solvent was present. A 5−10 mg sample was purged with nitrogen gas while heating. The balance experiments were conducted in a 100 mL three-neck flask fitted with stopcocks and a 10 cm ground-glass tube on the center neck. A stainless steel wire was hung from the hook arm underneath the

(12) Buss, C. E.; Anderson, C. E.; Pomije, M. K.; Lutz, C. M.; Britton, D.; Mann, K. R. *J. Am. Chem. Soc.* **1998**, *120*, 7783.
(13) Exstrom, C. L.; Sowa, J. R., Jr.; Daws, C. A.; Janzen, D. E.; Mann, D. R. *Chem. Mater.* **1995**, *7*, 15.
(14) Mann, K. R.; Daws, C. A.; Exstrom, C. L.; Janzen, D. E.; Pomije, M. K. (Regents of the University of Minnesota) U.S. Patent 5,766,952, 1998.
(15) Nagel, C. C. U.S. Patent 4,834,909, 1989.
(16) Exstrom, C. L. Ph.D. Dissertation, University of Minnesota, 1995.
(17) Fanizzi, F. P.; Intini, L.; Maresca, L.; Natile, G. *J. Chem. Soc., Dalton Trans.* **1990**, 199.
(18) Mason, W. R.; Gray, H. B. *J. Am. Chem. Soc.* **1968**, *90*, 5721.
(19) Ugi, I.; Meyr, R. *Org. Synth.* **1961**, *41*, 101.
(20) Anderson, C. E. Masters Thesis, University of Minnesota, 1997.
(21) Keller, H. J.; Lorentz, R. *J. Organomet. Chem.* **1975**, *102*, 119.

***Table 1.*** Crystal Data, Data Collection Details, and Refinement Parameters for Pt(CN-*p*-($C_2H_5$)$C_6H_4$)$_2$(CN)$_2$·0.5(toluene) (1) and Pt(CN-*p*-($C_2H_5$)$C_6H_4$)$_2$(CN)$_2$·*x*(hexanes) (2)

| | 1 | 2 |
|---|---|---|
| formula | $C_{23.5}H_{22}N_4Pt$ | $C_{20}H_{18}N_4Pt$[a] |
| habit, color | needle, yellow | needle, yellow |
| size, mm | 0.30 × 0.10 × 0.10 | 0.35 × 0.13 × 0.07 |
| lattice type | monoclinic | monoclinic |
| space group | *C*2/*c* | *C*2/*c* |
| *a*, Å | 19.893(1) | 20.094(1) |
| *b*, Å | 18.365(1) | 18.243(1) |
| *c*, Å | 13.150(1) | 13.141(1) |
| $\beta$, deg | 118.127(1) | 117.813(1) |
| *V*, Å$^3$ | 4237.1(4) | 4260.6(3) |
| *Z* | 8 | 8 |
| fw | 555.54 | 509.47[a] |
| $D_c$, g cm$^{-3}$ | 1.742 | 1.589[a] |
| $\mu$, mm$^{-1}$ | 6.639 | 6.594[a] |
| *F*(000) | 2152 | 1952[a] |
| $\theta$ range, deg | 1.61−25.01 | 1.60−25.05 |
| index ranges | $-23 \le h \le 20$, $0 \le k \le 21$, $0 \le l \le 15$ | $-23 \le h \le 21$, $0 \le k \le 21$, $0 \le l \le 15$ |
| no. of rflns collected | 9918 | 9183 |
| no. of unique rflns | 3687 ($R_{int}$ = 0.0274) | 3683 ($R_{int}$ = 0.0357) |
| weighting factors:[b] *a*, *b* | 0.0307, 3.4971 | 0.0406, 0.0000 |
| extinction coeff | 0.000 37(3) | 0.000 10(3) |
| max, min transmissn | 0.514, 0.136 | 0.630, 0.099 |
| no. of data, restraints, params | 3687/41/252 | 3683/30/229 |
| R1, wR2 ($I > 2\sigma(I)$) | 0.0318, 0.0631 | 0.0420, 0.0848 |
| R1, wR2 (all data) | 0.0703, 0.0732 | 0.1055, 0.1023 |
| goodness of fit (on $F^2$) | 1.032 | 0.932 |
| largest diff peak, hole, e Å$^{-3}$ | 0.802, −0.485 | 1.753, −1.179 |

[a] These items do not take into account the electron density of the disordered solvent molecule. [b] $w = [\sigma^2(F_o^2) + (aP)^2 + (bP)]^{-1}$, where $P = (F_o^2 + 2F_c^2)/3$.

balance and attached to a holder designed for a 1 cm diameter aluminum pan. Samples (15−30 mg) were placed in the pan, set on the holder, and suspended down the tube into the flask. After the sample was purged with pure nitrogen, the nitrogen stream was bubbled through the liquid VOC. Sample mass was recorded as a function of time.

**X-ray Structure Determination of Pt(*p*-CN-$C_6H_4C_2H_5$)$_2$(CN)$_2$·*x*(hexanes).** Crystals were grown by slow evaporation from a $CH_2Cl_2$/hexanes mixture. A crystal was attached to a glass fiber and mounted on the Siemens SMART CCD platform system[22] fitted with a graphite monochromator for data collection at 173(2) K with Mo K$\alpha$ ($\alpha$ = 0.710 73 Å) radiation. Crystal and X-ray collection and refinement data are summarized in Table 1.

The space group *C*2/*c* was determined on the basis of systematic absences and intensity statistics. A direct-methods solution provided the positions of most non-hydrogen atoms. Several full-matrix least-squares/difference Fourier cycles were performed to locate the positions of the remaining light, non-hydrogen atoms. The structure was found to contain channels filled with disordered solvent molecules. Attempts to model the disordered hexanes failed; the R1 value of the structure without modeling the solvent was R1 = 5.00%. Additional information about the solvent channels was obtained using the Platon/Squeeze programs.[23] The channels were found to occupy 796.0 Å$^3$, or 17.8% of the total unit cell volume. A total electron count of 304.2 e (approximately six hexanes) was found to occupy the channels. The original data were corrected for the disordered solvent, and the structure was refined to give a final R1 = 4.20%. The empirical formula, $F_{000}$, formula weight, and absorption coefficient are all known to be incorrect, since no solvent was taken into consideration in those calculations.

All non-hydrogen atoms were refined with anisotropic displacement parameters. Hydrogen atoms were placed in idealized positions and refined as riding atoms with isotropic relative displacement parameters. Additionally, the phenyl rings of the isocyanide ligands were refined as rigid bodies. Several atoms had large anisotropic displacement parameter maximum/minimum ratios: in particular, N3 and several carbon atoms on the phenyl rings.

(22) Siemens SMART Platform CCD; Siemens Industrial Automation, Inc., Madison, WI.
(23) Spek, A. L. *Acta Crystallogr*. **1990**, *A46*, C34.

***Table 2.*** Bond Lengths (Å) and Selected Bond Angles (deg)[a] for Pt(CN-*p*-($C_2H_5$)$C_6H_4$)$_2$(CN)$_2$·0.5(toluene) (1) and Pt(CN-*p*-($C_2H_5$)$C_6H_4$)$_2$(CN)$_2$·*x*(hexanes) (2)

| | 1 | 2 |
|---|---|---|
| Pt(1)−C(3) | 1.992(7) | 1.983(10) |
| Pt(1)−C(12) | 1.977(6) | 1.989(11) |
| Pt(1)−C(1) | 2.001(7) | 1.998(10) |
| Pt(1)−C(2) | 2.010(7) | 2.014(11) |
| N(1)−C(1) | 1.144(7) | 1.129(11) |
| C(2)−N(2) | 1.138(7) | 1.136(12) |
| C(3)−N(3) | 1.129(7) | 1.137(11) |
| N(3)−C(4) | 1.404(8) | 1.411(11) |
| N(4)−C(12) | 1.143(7) | 1.143(12) |
| N(4)−C(13) | 1.410(7) | 1.398(11) |
| C(4)−C(5) | 1.386(8) | 1.362(13) |
| C(4)−C(9) | 1.378(8) | 1.403(12) |
| C(5)−C(6) | 1.389(8) | 1.357(13) |
| C(6)−C(7) | 1.387(8) | 1.382(13) |
| C(7)−C(8) | 1.376(8) | 1.369(13) |
| C(7)−C(10) | 1.508(8) | 1.558(12) |
| C(8)−C(9) | 1.398(8) | 1.385(12) |
| C(10)−C(11) | 1.501(9) | 1.448(14) |
| C(13)−C(14) | 1.391(9) | 1.355(13) |
| C(13)−C(18) | 1.373(8) | 1.384(12) |
| C(14)−C(15) | 1.378(8) | 1.358(13) |
| C(15)−C(16) | 1.389(8) | 1.419(12) |
| C(16)−C(17) | 1.381(9) | 1.375(14) |
| C(16)−C(19) | 1.505(8) | 1.532(13) |
| C(17)−C(18) | 1.376(8) | 1.392(13) |
| C(19)−C(20) | 1.507(9) | 1.519(13) |
| C(3)−Pt(1)−C(12) | 91.0(4) | 91.3(2) |
| C(3)−Pt(1)−C(1) | 88.9(4) | 89.5(2) |
| C(12)−Pt(1)−C(1) | 177.7(4) | 177.6(2) |
| C(3)−Pt(1)−C(2) | 177.5(4) | 177.2(2) |
| C(12)−Pt(1)−C(2) | 91.4(4) | 90.8(2) |
| C(1)−Pt(1)−C(2) | 88.6(4) | 88.3(2) |

[a] Estimated standard deviations in the least significant figure are given in parentheses.

The asymmetric unit is one formula unit. The platinum atom was found to occupy a general position. The two largest peaks in the difference Fourier map with heights greater than 1 e/Å$^3$ are near the platinum atom: height 1.75 e/Å$^3$, 1.02 Å from Pt1; height 1.35 e/Å$^3$, 1.14 Å from Pt1. All calculations were performed with the SHELXTL V5.0 suite of programs.[24] Selected bond lengths and bond angles are given in Table 2.

**X-ray Structure Determination of Pt(*p*-CN-$C_6H_4C_2H_5$)$_2$(CN)$_2$·0.5(toluene).** Crystals were grown by slow evaporation from a $CH_2Cl_2$/toluene mixture. A crystal was attached to a glass fiber and mounted on the Siemens SMART CCD platform system.[22] Crystal and X-ray collection and refinement data are summarized in Table 1. Initially a subcell with $^1/_4$ the size of the *c* axis was indexed. Subsequently the data were reindexed and it was found that the cell conformed to the current *C*-centered monoclinic cell. The space group *C*2/*c* was determined on the basis of systematic absences and intensity statistics. The structure initially could not be solved in *C*2/*c* and was solved in *Cc*. A 2-fold axis was found, and the structure was transformed to the *C*2/*c* space group.

A direct-methods solution provided the positions of most non-hydrogen atoms. Several full-matrix least-squares/difference Fourier cycles were performed to locate the positions of the remaining light, non-hydrogen atoms. The structure was found to contain channels filled with disordered toluene molecules. The channels were found to occupy

(24) Sheldrick, G. M. SHELXTL, version 5.0; 1994.

773.3 Å$^3$, or 18.2% of the total unit cell volume. The toluene molecule found occupying the channel was disordered and was refined as a rigid body. A total of 41 restraints were used to refine the toluene molecule. The toluene molecule is disordered over an inversion center with each position having an occupancy of 0.5. Final refinement gave R1 = 3.17%.

All non-hydrogen atoms were refined with anisotropic displacement parameters. Hydrogen atoms were placed in idealized positions and refined as riding atoms with isotropic relative displacement parameters. The asymmetric unit is one formula unit. The platinum atom is located on a general position. There are no remaining electron density peaks greater than 1 e/Å$^3$ in the Fourier map. All calculations were performed with the SHELXTL V5.0 suite of programs.[24] Selected bond lengths and bond angles are given in Table 2.

**Powder X-ray Diffraction Data Collection.** Room temperature (23 °C) X-ray powder diffraction patterns were obtained with a Siemens D-5005 diffractometer with a 2.2 kW sealed copper source equipped with a single-crystal graphite monochromator, scintillation counter, and slits of [1°, 1°, 1°, 0.6°, 0.6°]. Powder diffraction patterns were collected from $2\theta = 2-60°$ with a $2\theta$ stepping angle of 0.02° and an angle dwell of 2 s.

The sample cell was constructed by gluing four glass microscope slide covers to a 45 mm × 45 mm × 3.2 mm glass plate. The slide covers were arranged to produce a 7.8 mm × 23.3 mm indentation 0.4 mm deep. This arrangement forms a thin sample well that requires a small sample size (~20 mg) and allows rapid equilibration of the compound with the solvent vapor. The sample powder was packed into the sample well and leveled off with a microscope slide.

Vapochromic X-ray experiments were carried out by enclosing the sample holder in a small, resealable plastic bag. The powder patterns collected with the sample inside the plastic bag show a slight increase in the baseline intensity but do not contain additional reflections in the $2\theta = 2-60°$ data collection range. The samples were exposed to VOCs by placing glass wool saturated with 5−10 mL of toluene in the bag, which was then sealed to create a room-temperature atmosphere saturated with the VOC vapors. The sample, toluene vapor, and liquid toluene were allowed to come to equilibrium. The equilibration period was monitored by collecting fast "snapshot" scans until the position of the reflections became constant. These "snapshot" scans (~10 min) were typically collected for $2\theta = 2-20°$ with slits of [1°, 1°, 1°, 0.6°, 0.6°], a $2\theta$ stepping rate of 0.05°, and an angle dwell of 1 s. As the VOC equilibrated with the sample, the reflections became increasingly broad because the sample surface buckles due to the increase in volume of the unit cell. Once the peak positions were stable, the sample was quickly removed from the bag and the surface of the sample was flattened. The sample was again placed in the bag with the VOC, "snapshot" scans were used to again check for equilibration, and a long scan was then collected. The sample was then removed from the bag and allowed to equilibrate with the room atmosphere. Again snapshot scans were used to determine when the positions of the reflections had become constant, and a long scan was collected. The sample was then allowed to sit in the laboratory atmosphere for approximately 1 week, and a final scan was then obtained.

Variable-temperature X-ray powder diffraction scans were obtained on a Scintag XDS200Theta/Theta diffractometer equipped with a high- and low-temperature apparatus and slits of [1°, 2°, 0.5°, 0.3°] moving from the source to the detector. Patterns were collected in the step-scanning mode from $2\theta = 2$ to $2\theta = 60°$ with a $2\theta$ step angle of 0.02° and an angle dwell time of 2 s. The sample material was exposed to the toluene vapor for several hours, packed into the sample holder, and allowed to equilibrate with the laboratory atmosphere. A long scan was collected, and then the sample was heated to 100 °C. Once the temperature set point was reached, the sample was allowed to equilibrate at that temperature for 30 min before the data collection was begun. A second postheating room-temperature long scan was collected. The sample holder consisted of a copper plate with a circular sample well. All powder diffraction data were processed using Jade v.3.0 software.[25]

**Infrared Spectroscopy.** Infrared spectra were obtained by the attenuated total reflectance (ATR) method with a Nicolet Magna-FTIR System 550 spectrometer equipped with a ZnSe trough HATR cell from PIKE Technologies. Data were processed with OMNIC ESP v. 4.1 software. Sample films were coated on the ZnSe crystal from either an ether suspension or a $CH_2Cl_2$ solution. For vapochromic experiments, a beaker filled with glass wool saturated with several milliliters of VOC was placed on the ZnSe mount and the ATR cell was then covered. Spectra were recorded as the equilibrium vapor pressure of the VOC was established, after the VOC source was removed, and after heating of the sample in a 100 °C oven.

**Emission Spectra.** Emission spectra were recorded at room temperature with a custom Princeton Instruments ST138 UV−vis/near-IR sensitive LN/CCD spectrometer. The Winspec v2.3.3 software package was used for acquiring the emission spectra. The emission spectra (front face detection from solids) were collected from samples irradiated at 435.8 nm with the interference-filtered output of an Oriel 100 W Hg arc lamp. The emission spectra were corrected for grating efficiency and detector response.[26] The emission efficiency was estimated to be similar to $Ru(bpy)_3Cl_2$ (bpy = 2,2′-bipyridine) by measuring the scattered excitation light and emitted light from a film of **O-PtC$_2$** and then from an optically dense solution of $Ru(bpy)_3Cl_2$ in methanol.[27]

A film of the **O-PtC$_2$** compound was coated onto a calcium fluoride window from an ether slurry and fitted into a flow-through cell. Heating tape was wrapped around the cell, and the temperature of the sample was monitored via a thermocouple that was placed to contact the sample film without interfering with the emission of the compound. A gas inlet and outlet located on the back of the cell were used to flow dry $N_2$ or VOC-saturated $N_2$ over the sample. During the exposure of the sample to the VOC a continuous series of spectra were collected. SPECFIT,[28] a spectral data analysis software package, was used to fit the spectral changes and to calculate the eigenspectra of the different uptake phases.

## Results

**Synthesis and Characterization.** The neutral **PtC$_2$** compound is synthesized in high yield by heating the precursor double-salt compound **4C$_2$** to the 201 °C melting point. Recrystallization of the resulting material results in either purple ($\lambda_{max}$ 570 nm) or orange ($\lambda_{max}$ 515 nm) products that are identical by elemental analysis and solution NMR. The purple product is easily obtained by rapidly adding excess hexanes to a $CH_2Cl_2$ solution of **PtC$_2$**. The orange product (**O-PtC$_2$**) is obtained in pure form by slow crystallization from $CH_2Cl_2$ solution, but it was more conveniently produced by slurrying **P-PtC$_2$** with THF to give a yellow solid. Heating this yellow compound to 110 °C and subsequent cooling to room temperature results in an orange product that NMR, FTIR, and X-ray powder diffraction show is identical with **O-PtC$_2$** obtained by crystallization from $CH_2Cl_2$.

Both **P-PtC$_2$** and **O-PtC$_2$** are stable in the laboratory atmosphere; thus, no special precautions were taken prior to any experiments. The possibility that **P-PtC$_2$** and **O-PtC$_2$** correspond to a cis/trans isomer pair was ruled out by thin-layer chromatography and subsequent physical studies (vide infra). Qualitative vapochromic tests indicated that **P-PtC$_2$** is not appreciably vapochromic, while **O-PtC$_2$** responded visually

(25) Jade V3.0 software; Materials Data Inc., Livermore, CA.
(26) The emission spectra were corrected to arbitrary units proportional to photons per energy. For this calculation see: Blasse, G.; Grabmier, B. C. *Luminescent Materials*; Springer-Verlag: Heidelberg, Germany, 1994; p A225.
(27) Caspar, J. V.; Meyer, T. J. *J. Am. Chem. Soc.* **1983**, *105*, 5583.
(28) SPECFIT: Binstead, R. A.; Zuberbühler, A. D. Specfit, version 2.09; Spectrum Software Associates, Chapel Hill, NC, 1995.

***Table 3.*** Emission $\lambda_{max}$, Vapochromic Shifts, and VOC Concentrations for Emission Studies of O−$PtC_2$

| VOC | $\lambda_{max}$ | vapochromic shift (nm)[a] | VOC concn mole fraction[b] |
|---|---|---|---|
| none | 611 | | |
| toluene | 565 | −46 | 0.0337 |
| benzene | 586 | −25 | 0.114 |
| chlorobenzene | 592 | −19 | 0.0142 |
| *p*-xylene | 585 | −26 | 0.0100 |
| mesitylene | 565 | −46 | 0.0028 |
| ethanol | 587 | −24 | 0.0689 |

[a] Vapochromic shift = $\lambda_{max}$(VOC) − $\lambda_{max}$(none). [b] The concentrations of each VOC in the $N_2$ stream calculated from the partial pressures at 296 K.

to a variety of solvents; consequently, studies focused on **O-$PtC_2$**.

**Vapochromic Luminescence Studies of O-$PtC_2$.** The solid-state emission spectrum of **O-$PtC_2$** in the dry state under a nitrogen atmosphere at room temperature shows an intense emission band at 611 nm. The emission spectra in air were in all respects identical with those measured under nitrogen. Solid **O-$PtC_2$** gave an emission intensity (after correcting for scatter) similar to an optically dense solution of $Ru(bpy)_3Cl_2$ in methanol. By analogy to the linear chain $M_2Pt(CN)_4$ and Pt-$(CNR)_4Pt(CN)_4$ compounds, we assign this emission band to a component of the d$\sigma$*−p$\sigma$ one-electron excitation.[10,11,13,29,30] Exposure of the compound to the VOC vapors studied here resulted in a shift of the emission band to higher energy and a decrease in the band intensity (Table 3). In all cases heating to 110 °C while purging the sample with $N_2$ completely removed the solvent and regenerated the original spectrum of dry **O-$PtC_2$**. The data for each solvent were taken after two or three exposure/heat/cool cycles. In all cases the process was found to be completely reversible and no detectable degradation or rearrangement of the compound to **P-$PtC_2$** occurred after many cycles. The same film was used for multiple solvent exposures. The exposure to toluene and mesitylene occurred with the formation of an observable intermediate, while exposure to benzene, xylene, chlorobenzene, and ethanol did not.

Changes in the emission spectrum of **O-$PtC_2$** during the exposure to toluene clearly show the two sorption processes. During the first sorption the emission spectrum shifts rapidly (ca. 5 s) to higher energy by 16 nm and the emission intensity at the maximum decreases by approximately 45%. The second sorption occurs on a slower time scale (ca. 2 min); the spectrum shifts to higher energy by 28 nm and the intensity decreases an additional 12%. Both shifts occur isosbestically (Figure 1). The two isosbestic points occur at approximately 535 and 562 nm. Specfit[28] was used to obtain emission spectra of the three different pure phases (Figure 2) involved in the toluene exposure. Similar results were obtained for the mesitylene exposure, but the emission maxima occur at different wavelengths (Table 3). The concentrations of the VOCs in the nitrogen stream were calculated from the partial pressure of each VOC at 296 K.[31] Results are summarized in Table 3.

In the case of toluene and mesitylene exposures, removal of the VOC causes the spectrum to quickly (minutes) reverse to the intermediate phase but reversal to the original spectrum requires heating or long-term (days) $N_2$ purging. In the case of benzene, xylene, chlorobenzene, and ethanol the original spectrum is obtained with heating.

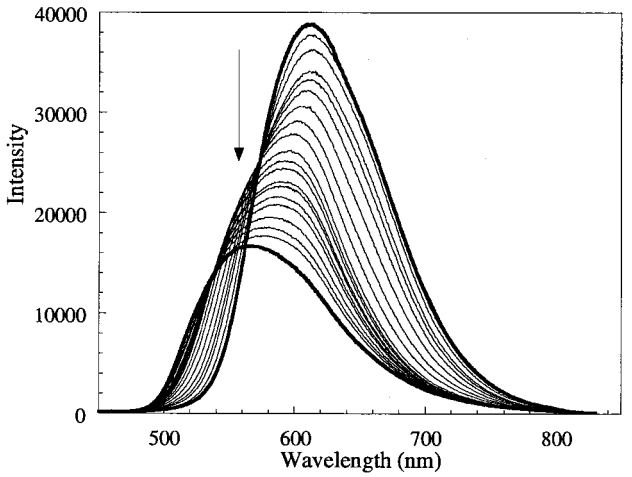


***Figure 1.*** Emission spectra excited at $\lambda$ 435.8 nm of a thin film of **O-$PtC_2$** as toluene vapor is admitted. The arrow shows the direction of intensity change. The first nine spectra are taken 0.6 s apart, the next five spectra are taken 2.0 s apart, and the final six spectra are taken 10 s apart.

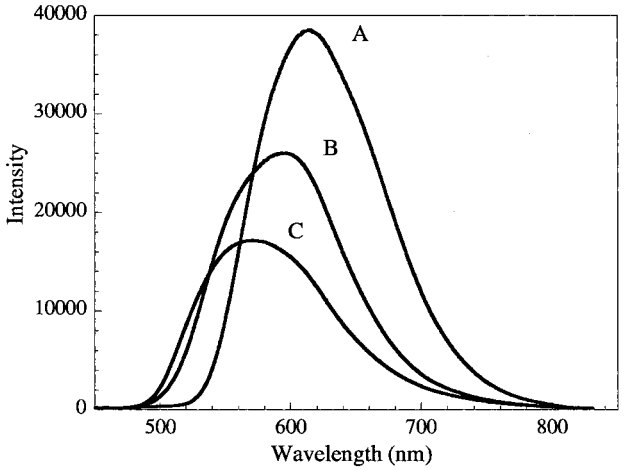


***Figure 2.*** Calculated pure component spectra from the data in Figure 1: (A) unexposed **O-$PtC_2$**; (B) **O-$PtC_2$**·0.25(toluene); (C) **O-$PtC_2$**·0.5(toluene).

***Table 4.*** FT-IR Data for P−$PtC_2$ and O−$PtC_2$ Exposed to Toluene

| compd | $\nu_{CNR}$ ($cm^{-1}$) | | $\nu_{CN}$ ($cm^{-1}$) | |
|---|---|---|---|---|
| **P-$PtC_2$** | 2251 | 2231 | 2157 | 2150 |
| **O-$PtC_2$**[a] | 2247 | 2229 | 2157 | 2150 |
| **O-$PtC_2$**[b] | 2246 | 2229 | 2159 | 2153 |
| **O-$PtC_2$**·0.25(toluene) | 2244 | 2229 | 2159 | 2153 |
| **O-$PtC_2$**·0.5(toluene) | 2244 | 2229 | 2159 | 2152 |

[a] Original preexposure sample. [b] After exposure to toluene.

**Vapochromic Infrared Studies.** We investigated the interactions between the VOC guest and the **O-$PtC_2$** host with ATR FTIR spectroscopy (Table 4). Previously, the C≡N stretching region (2100−2300 $cm^{-1}$) of the mid-IR has been shown to be sensitive to the presence of VOC guest molecules.[10−12] A film of **O-$PtC_2$** (deposited on the ATR crystal from an ether slurry) showed $\nu_{CN}$ stretches at 2157 and 2150 $cm^{-1}$ and $\nu_{CNR}$ stretches at 2247 and 2229 $cm^{-1}$. The observation of two bands each for $\nu_{CN}$ and $\nu_{CNR}$ is consistent with a cis geometry about the Pt center (confirmed by crystallography; vide infra). The orange

(29) Gliemann, G.; Yersin, H. *Struct. Bonding* **1985**, *62*, 87.
(30) Miskowski, V. M.; Houlding, V. H. *Inorg. Chem.* **1991**, 30, 4446.
(31) Nelson, G. O. *Gas Mixtures-Preparation and Control*; Lewis Publishers: Chelsea, MI, 1992.

film cast from ether was dissolved on the ATR plate with $CH_2Cl_2$, and when the solvent evaporated, a purple film remained. After the film was purged with $N_2$ for several minutes, the spectrum of the purple film exhibited $\nu_{CN}$ stretches at 2157 and 2150 $cm^{-1}$ and $\nu_{CNR}$ stretches at 2251 and 2231 $cm^{-1}$. The IR spectra of **O-PtC$_2$** and **P-PtC$_2$** are nearly identical. A second spectrum of the purple material was obtained from a film of **P-PtC$_2$** cast from an ether slurry. This spectrum was identical with that of the purple film resulting from the **O-PtC$_2$** film redissolved in $CH_2Cl_2$ and allowed to evaporate to dryness. Again, both the **P-PtC$_2$** and the **O-PtC$_2$** IR spectra are consistent with a cis geometry about the Pt metal center.

The first exposure of the dry **O-PtC$_2$** film to toluene vapor results in a rapid change at room temperature of the C≡N stretching region (Table 4). The full exposure to toluene occurs quickly, within approximately 2 min. Peaks for this species are at $\nu_{CN}$ 2159 and 2152 $cm^{-1}$ and $\nu_{CNR}$ 2244 and 2229 $cm^{-1}$. The peak area of the CNR region increased by 28%, and the peak area of the CN region increased by 40% upon exposure of the dry sample to toluene vapors. Additional equilibration time with the toluene vapor for 1 h gave no further changes. Removal of the toluene vapor gave a rapid spectral change (2 min) to an intermediate phase that is stable under nitrogen for more than 1 h. This intermediate phase has peaks at $\nu_{CN}$ 2159 and 2153 $cm^{-1}$ and $\nu_{CNR}$ 2229 $cm^{-1}$. The peak area of the CNR stretching region decreased 28% as compared to the toluene-exposed sample, returning to the intensity of the original dry sample. However, the peak area of the CN region decreased by only 20%, or half of the original increase. Cycling between the intermediate and full exposure spectra occurs rapidly and very reversibly. The complete removal of toluene from the **O-PtC$_2$** film requires heating the sample to 100 °C with an $N_2$ purge to regenerate the spectrum of the dry sample (peaks at $\nu_{CN}$ 2159 and 2153 $cm^{-1}$ and $\nu_{CNR}$ 2246 and 2229 $cm^{-1}$). The complete cycle was repeated several times with identical results and with no noticeable degradation of the compound.

**Single-Crystal Structures of Pt(CN-*p*-($C_2H_5$)$C_6H_4$)$_2$(CN)$_2$.** Single-crystal data for **PtC$_2$**·0.5(toluene) and **PtC$_2$**·*x*(hexanes) are given in Table 1; selected bond lengths and angles are given in Table 2. The two crystal structures of **PtC$_2$** have nearly identical packing arrangements. Both structures consist of infinite stacks of cis geometry and planar molecules with chains of platinum atoms that are parallel to the *c* axis (Figure 3). Within the unit cell there are two crystallographically equivalent chains, one centered near $a = 0$, $b = 0$ and the other related by the *c* face centering, near $a = 0.5$ and $b = 0.5$. In each chain four molecules stack along the *c* axis per unit cell (Figure 4). The platinum atoms are all on general positions. The second **PtC$_2$** molecule in the chain is related to the first **PtC$_2$** molecule by a 2-fold axis parallel with the *b* axis and located at $^1/_4$ along the *c* axis, the third **PtC$_2$** molecule in the chain is related to the first **PtC$_2$** molecule by a *c* glide plane, and the fourth **PtC$_2$** molecule is related to the first **PtC$_2$** molecule by an inversion center positioned at $a = 0$, $b = 0$, $c = ^1/_2$. The average Pt−Pt separation in **PtC$_2$**·0.5(toluene) is 3.2905(2) Å, nearly identical with $c/4 = 3.288(2)$ Å. This structure packs with an alternating long and short Pt−Pt separation (3.281 and 3.300 Å). The average Pt−Pt separation in **PtC$_2$**·*x*(hexanes) is 3.287(2) Å (with $c/4 = 3.285(2)$ Å); this structure also packs with an alternating long and short Pt−Pt separation (3.278 and 3.296 Å). The chains

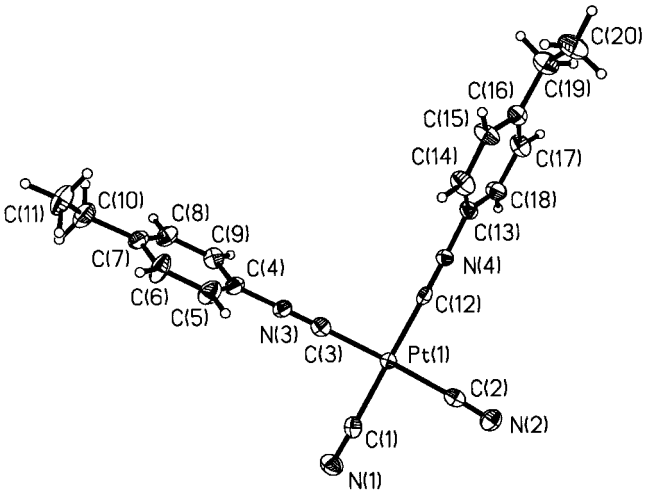


***Figure 3.*** ORTEP diagram showing one molecule of **O-PtC$_2$** from the **O-PtC$_2$**·0.5(toluene) crystal structure. Ellipsoids are drawn at the 50% level. The atom-numbering scheme for the **O-PtC$_2$**·*x*(hexanes) crystal is identical.

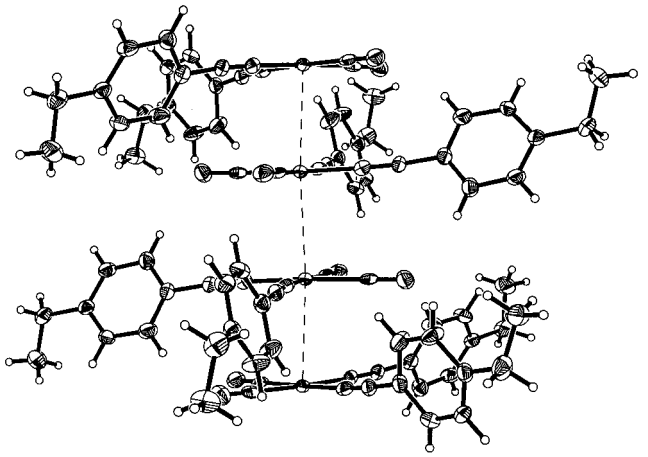

***Figure 4.*** Solid-state packing diagram of **O-PtC$_2$**·0.5(toluene) showing the Pt−Pt interactions.

of platinum atoms are slightly zigzagged, giving Pt−Pt−Pt angles of 175.5° in **PtC$_2$**·0.5(toluene) and 176.1° in **PtC$_2$**·*x*(hexanes). The location of the isocyanide ligands allows solvent channels parallel with the *c* axis. These channels are located at approximately $a = 0.5$, $b = 0$ and $a = 0$, $b = 0.5$ (Figure 5). Each channel occupies 387.5 $Å^3$ within one unit cell length. The total solvent-accessible volume occupies 18.2% of the total volume of the unit cell (or 193 $Å^3$ per toluene molecule for the **PtC$_2$**·0.5(toluene) structure).

**TGA and Gravimetric Studies.** TGA studies with both the purple and orange morphs of **PtC$_2$** showed that neither of these compounds lost significant mass or decomposed when heated to 150 °C. This result is consistent with no lattice solvent present in either compound. The purple morph was not investigated further.

Gravimetric studies with bulk samples (ca. 10 mg) show that exposure of **O-PtC$_2$** to toluene results initially in a very fast mass gain equivalent to 0.5(1) toluene molecules per **O-PtC$_2$** molecule over approximately 6 min. Additional exposure for long periods of time (hours) results in additional mass gain with a final mass equivalent to 0.9(1) toluene molecules per **O-PtC$_2$**. After the VOC source is removed from the **O-PtC$_2$** environment and the sample is purged with $N_2$, it quickly (5 min) loses weight

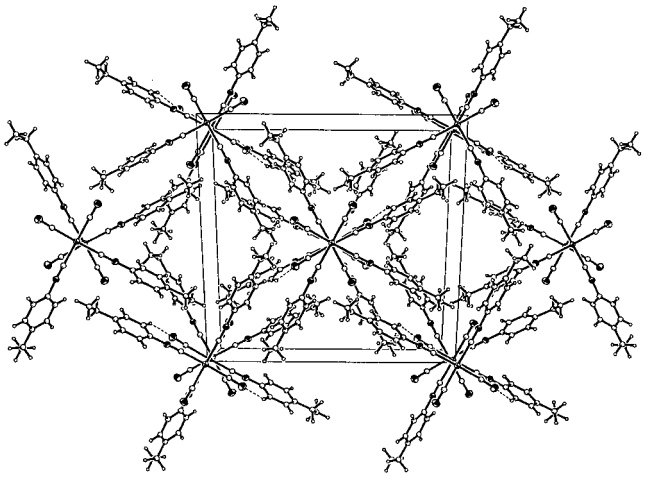

***Figure 5.*** Solid-state packing diagram of **O-PtC$_2$**·0.5(toluene). The view is down the *c* axis, showing the solvent channels parallel with the *c* axis. The toluene molecules were removed for clarity.

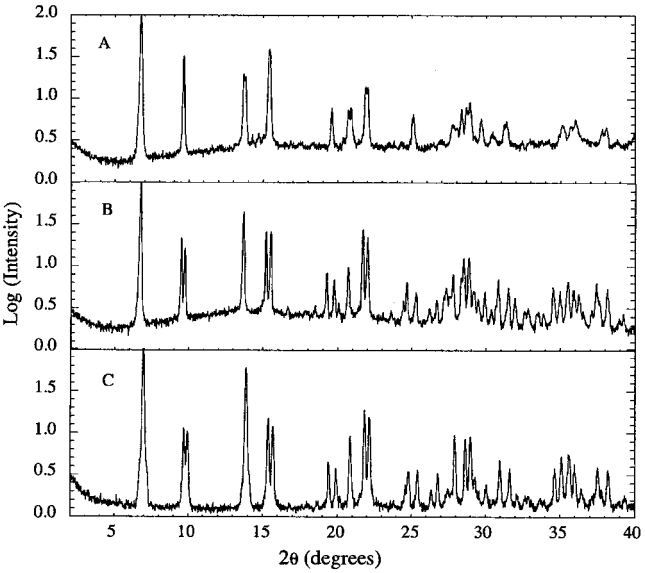


***Figure 6.*** X-ray powder diffraction patterns for **O-PtC$_2$**·*x*(toluene): (A) unexposed **O-PtC$_2$**; (B) **O-PtC$_2$**·0.25(toluene); (C) **O-PtC$_2$**·0.5(toluene).

until it reaches 0.5 equiv of toluene; at this point the rate of mass loss becomes dramatically slower, and with an additional 3 h of purging the sample reaches 0.25 equiv. Additional long-term $N_2$ purging is required to reach the original "dry" mass; heating speeds up the process significantly.

**Vapochromic Powder Diffraction Studies.** Repeated attempts to grow crystals of the "dry" orange and purple forms failed; therefore, these materials and the toluene-exposed materials were studied by X-ray powder diffraction. The powder pattern of **P-PtC$_2$** exhibits a single weak diffraction peak at approximately $2\theta = 7°$, indicating that this material has very little crystalline character. The $2\theta = 7°$ peak is most likely due to a small impurity of **O-PtC$_2$**, as it is very crystalline and exhibits its strongest diffraction peak near $2\theta = 7°$ (vide infra).

Powder diffraction data for **O-PtC$_2$** (Figure 6) were collected between $2\theta = 2°$ and $2\theta = 60°$. The resulting pattern is similar to the pattern generated from the single-crystal study of **PtC$_2$**·0.5(toluene); attempts to reindex the pattern in a higher crystal system failed. The single-crystal unit cell was input into the Cerius2 software[32] program, and the cell constants were varied until its predicted powder pattern matched that of the experimental pattern. Final indexing and cell refinement was done with Jade V 3.0 software,[25] and the results are given in Table 5. The resulting cell is monoclinic with $Z = 8$ and dimensions $a = 18.95(1)$ Å, $b = 17.89(1)$ Å, $c = 12.80(1)$ Å, and $\beta = 107.9(1)°$. Exposure of the dry **O-PtC$_2$** to toluene results in a color change from orange to yellow and changes in the powder diffraction pattern. The toluene-exposed **O-PtC$_2$** compound powder pattern was indexed to dimensions $a = 20.22(1)$ Å, $b = 18.29(1)$ Å, $c = 13.15(1)$ Å, and $\beta = 118.13(1)°$. This cell is nearly identical with that obtained for the single-crystal study and is assigned to the **PtC$_2$**·0.5(toluene) phase. Removal of the toluene vapor from the compound results in a third powder pattern but retention of the yellow color. The powder diffraction pattern of this intermediate was indexed to a cell with dimensions $a = 20.22(1)$ Å, $b = 18.29(1)$ Å, $c = 12.80(1)$ Å, $\beta = 118.13(1)°$. We suggest this powder pattern corresponds to the **O-PtC$_2$**·0.25(toluene) phase that is observed in the gravimetric studies. Finally, an exposed sample was heated to 100 °C for 30 min, and cooled, and a final powder pattern of the resulting orange material was taken. The powder pattern of the cooled sample is identical with that of the original preexposure sample. The unit cell data for the different phases of toluene exposure as well as for the single-crystal structures are found in Table 5.

## Discussion

Previous studies of the platinum double salts of the general formula $[Pt(CNR)_4][Pt(CN)_4]$ (R = aryl, alkyl) have shown that the color as well as the unit cell changes that occur upon uptake of VOC vapor molecules can be dramatic.[7−16] It is interesting that these ionic double salts are precursors for isomeric neutral compounds such as **PtC$_2$**, which also exhibit vapochromic behavior. The broad implication is that the packing of the insoluble salt and the corresponding soluble neutral species are similar enough to allow sorption but have significantly different behavior. Although the neutral compound studied here does not exhibit color (orange to yellow) or unit cell changes associated with the solvent vapor uptake as dramatic as the double salts, **O-PtC$_2$** has several important advantages as a potential sensor material. The neutral compound is thermodynamically stable to at least 120 °C, it does not respond appreciably to water or air, it is a crystalline phase so all of the solvent guest sites are identical crystallographically, and it is soluble in many common solvents, from which it can be cast as films.

A complicating factor for **PtC$_2$** is its existence as two different solid-state morphs. Purple **P-PtC$_2$** and orange **O-PtC$_2$** have equivalent solution NMR spectra, are identical by TLC, and have IR spectra indicating a cis geometry about the platinum center, eliminating the possibility that the two forms are a cis/trans isomer pair. The literature has several examples of similar neutral platinum compounds that exist in two differently colored forms.[30,33] Specifically, Pt(2,2′-bipyrimidine)$(CN)_2$, a compound that also forms linear chains of platinum atoms in the solid state, was found to have both a purple and a yellow form.[34] In this case the authors concluded that the color difference results from differing numbers of water molecules in the lattice. However,

(32) Cerius2 V3.0 software; Molecular Simulations Inc., San Diego, CA.
(33) Miskowski, V. M.; Houlding, V. H.; Che, C. M.; Wang, Y. *Inorg. Chem.* **1993**, *32*, 2518.
(34) Kiernan, P. M.; Ludi, A. *J. Chem. Soc., Dalton Trans.* **1978**, 1127.

***Table 5.*** Unit Cell Parameters and Packing Coefficients for O−$PtC_2$

| compd | *a* (Å) | *b* (Å) | *c* (Å) | *β* (deg) | *V* (Å$^3$) | $C_k$[c] |
|---|---|---|---|---|---|---|
| **$PtC_2$**·*x*(hexanes)[a] | 20.094(1) | 18.243(1) | 13.141(1) | 117.813(1) | 4260.6(3) | |
| **$PtC_2$**·0.5(toluene)[a] | 19.893(1) | 18.365(1) | 13.150(1) | 118.127(1) | 4237.1(4) | 0.692 |
| **O-$PtC_2$**[b] | 18.95(1) | 17.89(1) | 12.80(1) | 107.9(1) | 4129(1) | 0.620 |
| **O-$PtC_2$**·0.25(toluene)[b] | 20.22(1) | 18.29(1) | 12.80(1) | 118.13(1) | 4175(1) | 0.658 |
| **O-$PtC_2$**·0.5(toluene)[b] | 20.22(1) | 18.29(1) | 13.15(1) | 118.13(1) | 4289(1) | 0.684 |

[a] Data obtained from single-crystal X-ray diffraction studies at 173 K. [b] Room-temperature powder diffraction data. [c] Kitaigorodsky packing coefficients are calculated from [*Z* (mol vol)]/*V*.

in the case of **P-$PtC_2$** and **O-$PtC_2$**, TGA experiments and elemental analyses indicate that neither compound includes lattice solvent. In addition to their electronic absorption and emission spectra, the most significant difference between **P-$PtC_2$** and **O-$PtC_2$** is in their level of crystallinity. Powder diffraction experiments show that **P-$PtC_2$** is amorphous, while **O-$PtC_2$** is crystalline. It is proposed that the difference in color between **P-$PtC_2$** and **O-$PtC_2$** is due to different solid-state packing arrangements, including what must be large differences in the Pt−Pt distance. Fortuitously, it was the crystalline **O-$PtC_2$** compound that was found to be vapochromic, and further efforts were focused accordingly.

Gravimetric studies show that even bulk samples of microcrystalline **O-$PtC_2$** quickly sorb 0.5(1) molar equiv of toluene when exposed to toluene vapor. Samples continue to pick up additional mass but at a much slower rate until, at very long exposure times, 0.9(1) equiv of toluene is sorbed. The binding of toluene in this phase is very weak, and the phase was not studied further. When the toluene vapor source is removed, the mass loss is rapid and reaches a metastable state at 0.5 equiv of toluene. With continued $N_2$ purging, the sample slowly continues to lose weight until it reaches ca. 0.25 equiv. The remaining 0.25 equiv of toluene is held tenaciously and requires heating and purging for complete removal.

The powder diffraction studies show that the unit cell of **O-$PtC_2$** expands slightly upon exposure to toluene vapor and, upon removal of the toluene source, the unit cell contracts again. During the unit cell expansion all three axes increase significantly in length; however, this expansion is counteracted somewhat by a significant increase in the monoclinic angle. In harmony with the gravimetric experiments, this expansion occurs in two distinct steps from the initial dry phase; the **O-$PtC_2$**·0.25(toluene) phase is formed first and then the **O-$PtC_2$**·0.5(toluene) phase is formed (Figure 6). The 0.25(toluene) phase is not observed by the relatively slow diffraction experiments in the forward direction, but it is observed upon removal of the toluene vapor source. Release of toluene from **O-$PtC_2$**·0.25(toluene) to regenerate the original unit cell requires either heating or several days of purging.

Analysis of the three monoclinic unit cells involved in the sorption process reveal that the exposed material has the same unit cell dimensions as the single-crystal structure of **O-$PtC_2$**·0.5(toluene). A Connelly analysis[35] of the dry **O-$PtC_2$** unit cell indicates that there is 1569 Å$^3$ of free volume within the unit cell and a packing coefficient ($C_k$) of 0.620 (Table 5). The $C_k$ value of dry **O-$PtC_2$** is at the low end of the normal range for packing coefficients of organic molecules (0.595−0.887).[36] As determined by gravimetric analysis, four toluene molecules, with a volume of 372 Å$^3$, enter the unit cell to form **O-$PtC_2$**·0.5(toluene), but the unit cell volume increases by only 160 Å$^3$, or 43% of the required volume. The packing coefficient calculated for **O-$PtC_2$**·0.5(toluene) is 0.684, indicating that the uptake of toluene vapor gives a 10% increase in packing efficiency. An increase in the packing efficiency is the primary method that provides space for the incorporated solvent molecules. In sharp contrast, the vapochromic [Pt(CN-*iso*-$C_3H_7)_4$][$Pt(CN)_4$] (**$PtiC_3$**) double-salt compound previously reported is also poorly packed ($C_k = 0.622$), and the uptake of solvent molecules also results in a small (6% or less) change in packing efficiency.[12] However, in the **$PtiC_3$** case, the small increase in packing efficiency accompanies a very dramatic change in the unit cell volume (54% to 95% increases in volume, depending on the solvent). In summary, **O-$PtC_2$** sorbs vapors by allowing guest solvent molecules into preexisting pockets while **$PtiC_3$** responds by allowing the guest to form new volume.

A possible explanation for the disparity in expansion behavior between **$PtiC_3$** and **O-$PtC_2$** is a difference in guest−host interactions. Consistent with the low value of α, Abraham's H-bonding parameter,[37] and our previous study,[11] the sorption of toluene causes only 1 cm$^{-1}$ shifts in the $\nu_{CN}$ stretching frequency. In contrast, the crystal structure of **$PtC_2$**·0.5(toluene) also shows that there are no direct interactions between the guest toluene molecules and the cyanide ligands (the closest $N_{cyanide}\cdots H_{toluene}$ distance is 5.50(1) Å). The single-crystal structure of **$PtiC_3$**·$16H_2O$ clearly shows a network of hydrogen bonding with $N_{cyanide}\cdots H_{water}$ distances of approximately 2.8 Å. It is possible that the special molecular arrangements required for hydrogen-bonding networks between the anion and the included solvent allow the large unit cell expansions observed for **$PtiC_3$**.

The lack of important H-bonding interactions between the host and guest suggested that changes in the Pt−Pt distance might explain the vapoluminescent shifts observed for **O-$PtC_2$**. Powder diffraction studies reveal that, upon exposure to toluene vapor, the *c* axis of the **O-$PtC_2$** unit cell increases by 0.35 Å to give a Pt−Pt separation increase of about 0.09 Å. The increase in distance produces weaker interactions between the $d_{z^2}$ and $p_z$ orbitals of neighboring Pt atoms that result in a greater HOMO to LUMO energy gap.[30] The shifts to higher energy observed for the emission spectra of **O-$PtC_2$**·0.25(toluene) and **O-$PtC_2$**·0.5(toluene) are consistent with the Pt−Pt distance lengthening. Emission spectra for several additional **O-$PtC_2$**·VOC adducts (mesitylene, chlorobenzene, benzene, ethanol, and *p*-xylene) also show reversible changes. It is interesting that the two VOCs that cause the largest shifts in the emission spectrum of **O-$PtC_2$** (toluene and mesitylene) are not the largest, most polar, or most volatile VOCs. There is no obvious relationship between the magnitude of the vapochromic shift and any one VOC molecular

(35) Connelly volume calculations were completed using Cerius2 software.
(36) Kitaigorodskii, A. I. *Organic Chemical Crystallography*; Consultants Bureau Enterprises: New York, 1961; p 107.
(37) Abraham, M. H. *Chem. Soc. Rev.* **1993**, 73.

parameter. We cautiously suggest that the shifts caused by the VOC guest may couple the molecular shape to the Pt−Pt distance. More experiments with a larger variety of VOCs will be needed to elucidate the vapochromic mechanism for this compound.

## Conclusions

The single-crystal structure of **O-PtC$_2$**·0.5(toluene) shows that the cis geometry neutral complex crystallizes in a monoclinic space group and has a structure related to the double-salt materials $[Pt(CNR)_4][Pt(CN)_4]$. The structure packs with linear chains of Pt atoms and solvent channels parallel with the *c* axis. Powder diffraction studies show that solvent-free **O-PtC$_2$** also crystallizes in a monoclinic space group and the unit cell parameters of the exposed material are almost identical with those obtained from the single-crystal study. Gravimetric studies indicate that when **O-PtC$_2$** is exposed to toluene vapor 0.5 equiv is easily incorporated into the unit cell, but the reverse process occurs slowly, in two stages. The unit cell changes that occur when **O-PtC$_2$** is exposed to toluene vapor are accompanied by large, reversible blue shifts in the emission spectrum. Similar shifts that also occur for benzene, chlorobenzene, mesitylene, *p*-xylene, and ethanol are consistent with a lengthening of the average Pt−Pt distance. Overall, $Pt(CN\text{-}p\text{-}(C_2H_5)C_6H_4)_2(CN)_2$ is a very stable, vapoluminescent compound that has highly reversible and reproducible emission spectra.

**Acknowledgment.** K.R.M. acknowledges the financial support of the National Science Foundation under Grant No. CHE-9307837. We also acknowledge the single-crystal X-ray diffraction facility of the Chemistry Department at the University of Minnesota for the use of their Siemens SMART CCD platform system.

**Supporting Information Available:** X-ray crystallographic files in CIF format for $Pt(CN\text{-}p\text{-}(C_2H_5)C_6H_4)_2(CN)_2$·*x*(hexanes) and $Pt(CN\text{-}p\text{-}(C_2H_5)C_6H_4)_2(CN)_2$·0.5(toluene), additional references for footnote 6, emission spectra for **O-PtC$_2$** exposures to benzene, *p*-xylene, mesitylene, chlorobenzene, and ethanol, and powder diffraction data for four patterns. This material is available free of charge via the Internet at http://pubs.acs.org.

JA011986V